

1 Highlights from PHENIX - II

2 **Terry C. Awes (for the PHENIX Collaboration ‡)**

3 Oak Ridge National Laboratory, Oak Ridge, TN 37831 USA

4 E-mail: awes@mail.phy.ornl.gov

5 **Abstract.**

6 This contribution highlights recent results from the PHENIX Collaboration at
7 RHIC with emphasis on those obtained through lepton and photon measurements
8 in PHENIX.

9 Submitted to: *J. Phys. G: Nucl. Phys.*

10 **1. Introduction**

11 Following the discovery of the surprising "perfect liquid" properties of the dense
12 matter being produced in heavy ion collisions at RHIC [1], effort has intensified to
13 quantify the detailed characteristics of that matter. Photons and leptons are of special
14 interest because they are penetrating probes that do not undergo strong interactions
15 and therefore are unlikely to interact with the dense matter after their production.
16 Thus, they carry information about the system at the time of their production,
17 throughout the entire evolution of the collision. The PHENIX experiment at RHIC was
18 designed with emphasis on the measurement of leptons and photons, with electron and
19 photon identification at mid-rapidity, and muon spectrometers at forward and backward
20 rapidities (see [2] for a description of PHENIX).

21 As a result of their weaker electromagnetic coupling, lepton and photon production
22 are rare processes that require large data samples for precise measurements. As
23 a consequence of their low production rate the measurements are also subject to
24 large backgrounds. In the case of directly radiated photons, the backgrounds are
25 mostly photons from radiative decays of long-lived neutral mesons, predominantly
26 the abundantly produced neutral pions. In the case of the electron measurement the
27 background is mostly the internal or external conversion of these radiative decay photons
28 into electron-positron pairs, and in the case of the muon measurements it is the weak
29 decay of charged pions into muons.

30 With the 8th RHIC Run period recently completed, many of the new results reported
31 by PHENIX are improved measurements of previously published results obtained from

‡ A list of members of the PHENIX Collaboration can be found at the end of this issue

32 the smaller data sets of the earlier RHIC runs. This is particularly true of the lepton and
 33 photon measurements. As an example, due to the factor of 10 increase in the PHENIX
 34 Run 4 data sample compared to Run 2, the measurement of the neutral pion spectra
 35 in Au+Au collisions has been extended to nearly 20 GeV/c transverse momentum with
 36 decreased statistical and systematic errors [3]. This directly translates into improved
 37 direct photon and non-photonic electron measurements.

38 2. Parton Energy Loss

39 One of the most exciting early results from RHIC was the observed strong suppression of
 40 neutral pion production in central Au+Au collisions [4] compared to expectations from
 41 scaled p+p collisions, and the lack of suppression of the direct photon yield [5]. This
 42 strongly supported the conclusion that the initial collisions occurred at the expected
 43 rate, as evidenced by the expected direct photon yield, but that the neutral pions were
 44 suppressed due to strong interactions and energy loss of the initially scattered parton
 45 as it traversed the dense medium prior to fragmentation into particles like the pion.

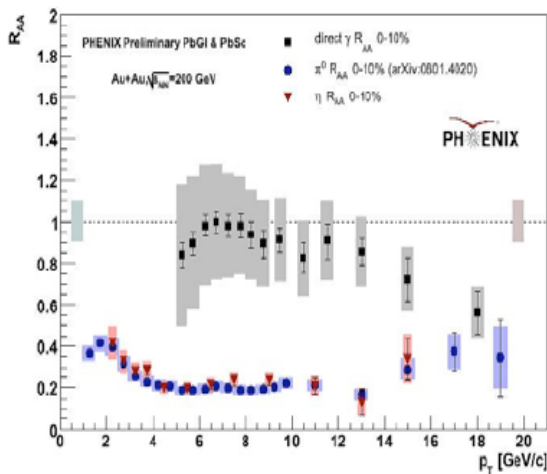


Figure 1. Nuclear modification factor R_{AA} for π^0 , η , and direct γ production as a function of transverse momentum for central Au+Au collisions.

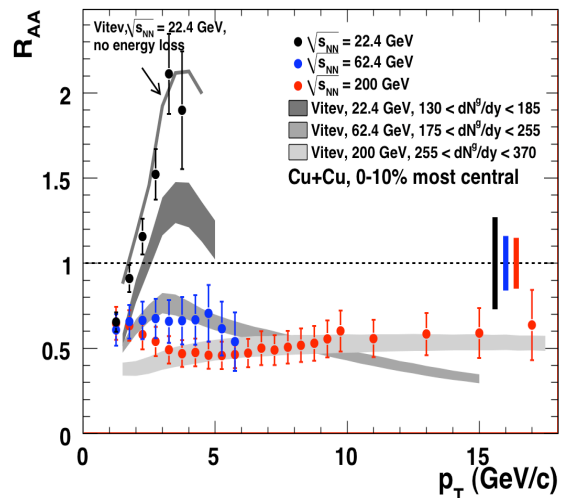


Figure 2. Nuclear modification factor R_{AA} for π^0 production in Cu+Cu collisions at $\sqrt{s_{NN}} = 22.4, 62.4,$ and 200 GeV. The shaded regions are parton energy loss model predictions [7].

46 Nuclear effects are quantified in terms of the nuclear modification factor R_{AB} defined
 47 as $R_{AB} = (dN/dp_T|_{A+B}) / (\langle N_{coll} \rangle \times dN/dp_T|_{p+p})$ where $\langle N_{coll} \rangle$ is the average number of
 48 independent nucleon-nucleon collisions for the selected class of events. Final results from
 49 analysis of the Run 4 data set shown in Figure 1 demonstrate that the π^0 suppression,
 50 and η suppression as well, is consistent with being constant with transverse momentum
 51 over the region from 5 to 20 GeV/c [3].

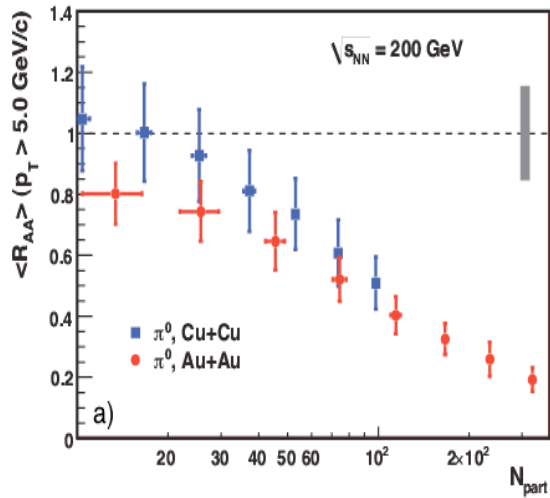


Figure 3. Nuclear modification factor R_{AA} for high $p_T \pi^0$ production as a function of the number of participant nucleons in Cu+Cu and Au+Au collisions.

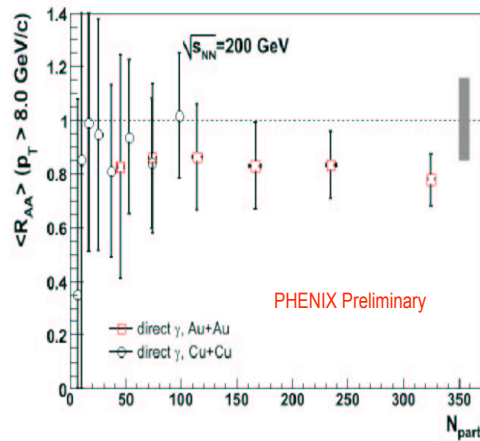


Figure 4. Nuclear modification factor R_{AA} for high p_T direct γ production as a function of the number of participant nucleons in Cu+Cu and Au+Au collisions.

52 New PHENIX results from Run 5 indicate that the neutral pion suppression is
 53 similar for Cu+Cu and Au+Au collisions for centrality selections with the same number
 54 of participating nucleons, as shown in Figure 3 [6]. On closer inspection, systematic
 55 differences between the Cu+Cu and Au+Au systems do appear at small participant
 56 numbers where differences in the geometry of the nuclear overlap may become important.

57 The dependence of the pion suppression on collision energy ($\sqrt{s_{NN}}$) has also been
 58 investigated with the Cu+Cu π^0 measurements where it is seen in Figure 2 that the
 59 suppression is quite similar at 200 and 62.4 GeV, but that the π^0 yield is instead
 60 enhanced compared to expectations from p+p collisions at 22.4 GeV, which indicates
 61 that suppression due to parton energy loss begins to dominate over Cronin enhancement
 62 between 22 and 62 GeV [6]. The $\sqrt{s_{NN}}$ dependence of the observed suppression is in
 63 good agreement with parton energy loss calculations [7].

64 As expected from previous observations, the high p_T direct photon yields are
 65 consistent within errors with no suppression for all centralities for both Cu+Cu and
 66 Au+Au collisions, as shown in Figure 4. The systematic study of the measured
 67 high p_T suppression of the single particle yields with varying particle species type
 68 (including heavy flavor), collision system centrality and $\sqrt{s_{NN}}$ will provide important
 69 input to model descriptions from which information about the opacity of the produced
 70 matter may be deduced by quantitative comparisons of the model predictions with the
 71 data [8, 9]. Beyond inclusive particle measurements, the parton energy loss is being
 72 further investigated through studies of high p_T direct photon v_2 measurements [10] and
 73 π^0 production as a function of the orientation with respect to the reaction plane [11],
 74 via two- and three-hadron correlations [2] as well as through γ -hadron correlations [12].

75 3. J/ψ Production

76 One of the earliest proposed signatures of the formation of dense deconfined matter
 77 (Quark Gluon Plasma) in relativistic heavy ion collisions was the predicted suppression
 78 of the J/ψ yield due to Debye screening of the $c\bar{c}$ quark bound state in the dense
 79 partonic matter [13]. Suppression of the J/ψ yield was soon afterwards observed in
 80 measurements at the CERN SPS [14]. New results from PHENIX [15] shown in Figure 5
 81 indicate that the J/ψ suppression is the same for Cu+Cu and Au+Au collisions for
 82 centrality selections with the same number of participating nucleons [16]. The amount
 83 of suppression increases with the number of participating nucleons and surprisingly is
 84 rather similar at RHIC and SPS energies [17]. Also, contrary to expectations from
 85 Debye screening alone, the suppression is observed to be stronger at forward rapidity
 86 than at mid-rapidity (Figure 5).

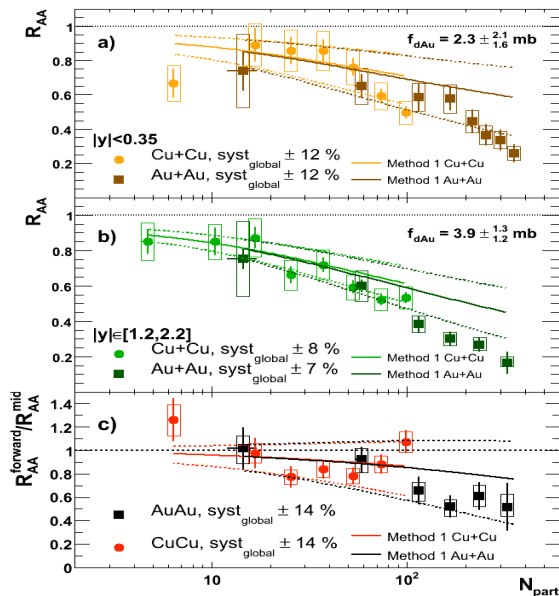


Figure 5. Nuclear modification factor R_{AA} as a function of the number of participant nucleons for Au+Au and Cu+Cu collisions at a) mid-rapidity and b) forward rapidity, and c) ratio.

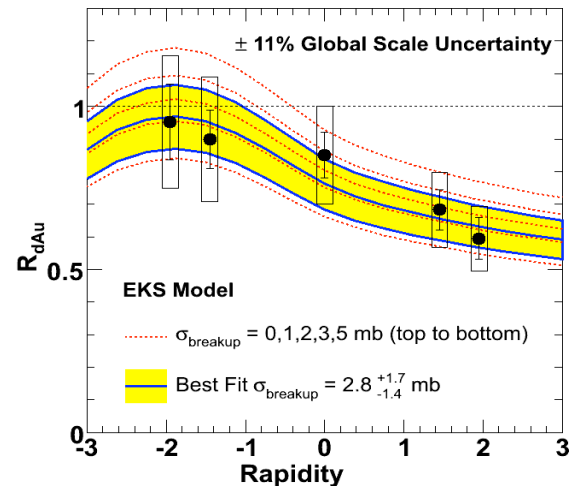


Figure 6. Nuclear modification factor R_{dAu} as a function of rapidity for J/ψ production in d+Au collisions compared to EKS model calculations [18].

87 At SPS energies the J/ψ yield is suppressed also in p+A collisions. This is
 88 interpreted as a cold nuclear matter (CNM) effect as a result of modification of the
 89 nucleon parton momentum distributions in the nucleus and the breakup of the J/ψ due
 90 to its interaction with the cold spectator nucleons. PHENIX has investigated the cold
 91 nuclear matter effects on J/ψ suppression at RHIC energies using d+Au collisions, with
 92 comparison to p+p collisions. A new analysis was recently completed using the Run 5
 93 p+p data set, which is a factor of 10 larger than the Run 3 p+p data set, together with
 94 the Run 3 d+Au data set. An improved analysis with better understanding of detector

95 effects has been applied consistently to both data sets. As shown in Figure 6 the new
 96 result on the d+Au nuclear modification factor R_{dAu} still has a rather large uncertainty
 97 that prevents to draw firm quantitative statements on any additional suppression in
 98 Au+Au collisions beyond cold nuclear matter effects (see Figure 5) [19, 20]. With the
 99 PHENIX Run 8 d+Au data sample just obtained it is estimated that the number of
 100 J/ψ 's accumulated is a factor of 50 greater than for Run 3, which should allow to
 101 constrain the contribution from cold nuclear matter effects more strongly.

102 4. Heavy Flavor

103 First measurements on heavy flavor quark production in PHENIX via single electron
 104 measurements provided another surprising result at RHIC [21]. Although it was
 105 expected that heavy quarks should show less stopping than light quarks in dense
 106 partonic matter, and hence heavy quark jets should show less quenching, it was instead
 107 observed that the yield of electrons from heavy flavor at high transverse momentum
 108 was suppressed in Au+Au collisions with nearly the same suppression as observed for
 109 π^0 's. In addition, single electrons attributed to heavy flavor were observed to show
 110 large azimuthal asymmetries [21], with the single electron v_2 results recently extended
 111 to higher transverse momenta with the Run 7 Au+Au data set, as shown in Figure 7.
 112 Taken together, the results implied significant damping of the motion of heavy quarks
 113 as they propagate through the dense matter produced at RHIC. Together with model
 114 calculations these observations allow to extract information on the viscosity to entropy
 115 ratio, η/s , of the dense matter and draw the conclusion that the matter has an η/s ratio
 116 close to the conjectured lower bound of $\sim 1/4\pi$, essentially a "perfect liquid" [1, 22].

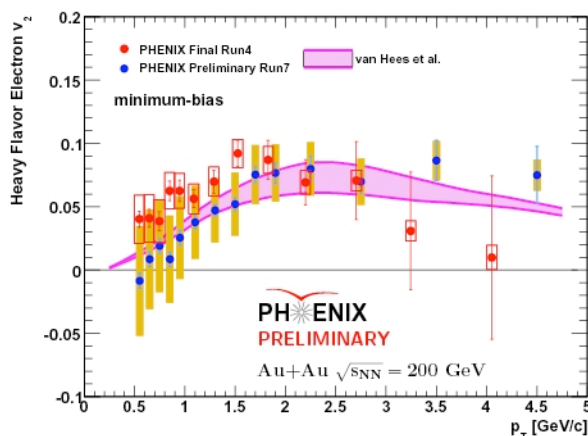


Figure 7. Azimuthal anisotropy parameter v_2 of heavy flavor electrons in minimum bias Au+Au collisions from Run 4 [21] and new preliminary results from Run 7 compared to transport calculations by van Hees [23].

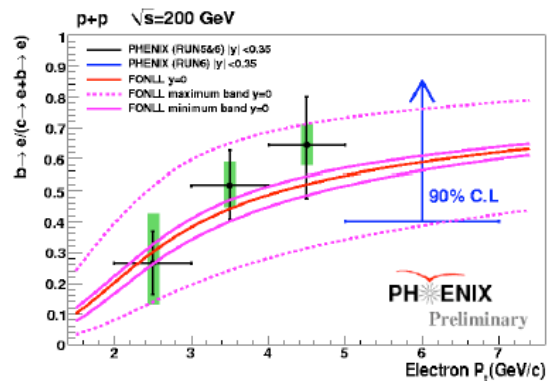


Figure 8. Ratio of electrons from bottom to electrons from charm compared to FONLL calculations [24].

117 With the goal to better separate the charm and bottom contributions (and
 118 shed light on the unresolved discrepancies between the STAR and PHENIX charm
 119 results) PHENIX has performed single muon measurements at forward rapidities
 120 in p+p collisions to extract information on the rapidity dependence of the heavy
 121 flavor production [25]. Also, electron-hadron correlation measurements have been
 122 used to perform a pseudo- D^0 analysis to explicitly separate the charm and bottom
 123 contributions [26] in p+p collisions with results shown in Figure 8. The measured ratio is
 124 found to be in good agreement with FONLL calculations, although separately the charm
 125 and bottom measurement each disagree significantly with the FONLL calculations [26].

126 5. Low Mass Electron Pairs

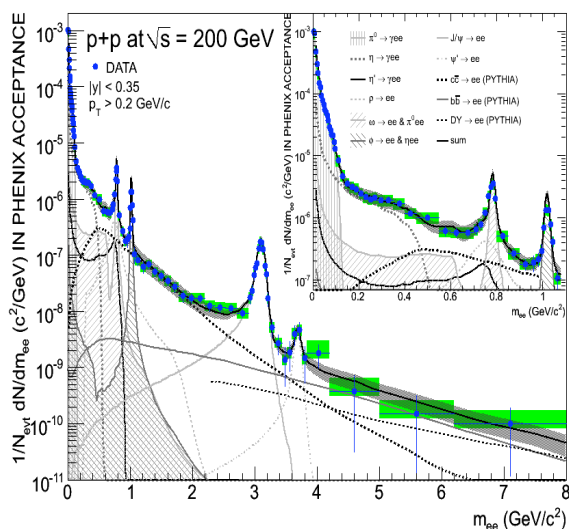


Figure 9. The yield of e^+e^- pairs per p+p collision compared to the yield expected from hadronic decays. Statistical (bars) and systematic (boxes) uncertainties are shown separately.

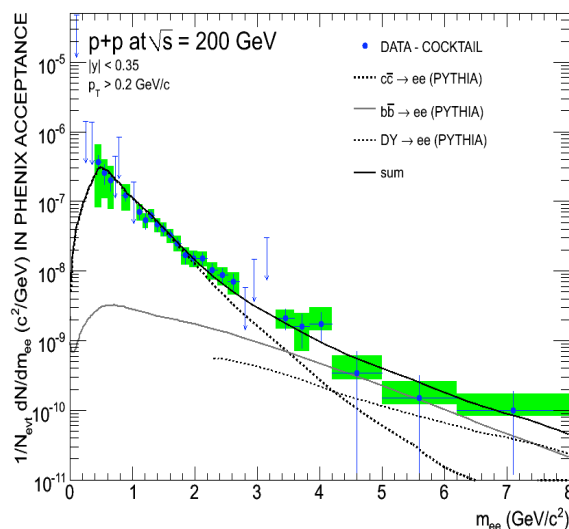


Figure 10. The yield of e^+e^- pairs after subtraction of the contribution of hadronic decays.

127 The measurement of electron-positron pairs allows the study of direct virtual photon
 128 production with the advantage that the main background from neutral pion decays (due
 129 to internal or external photon conversion) is about two orders of magnitude smaller than
 130 for the measurement of real direct photons. An additional order of magnitude reduction
 131 of the background to the virtual photon measurement can be obtained by using pairs
 132 with mass above the pion mass. The e^+e^- pair mass spectrum for p+p collisions at
 133 200 GeV from the PHENIX Run 5 data set [27] is shown in Figure 9. It is seen to be
 134 in very good agreement with the expected yield based on a Monte Carlo calculation of
 135 the electron-pair yield from hadron decays using measured hadron yields, together with
 136 contributions to the e^+e^- mass spectrum from Drell-Yan, $c\bar{c}$, and $b\bar{b}$ decays as predicted

137 by the PYTHIA model. Figure 10 shows the measured e^+e^- mass spectrum, after
 138 subtraction of the hadronic decay contribution, compared separately to the PYTHIA
 139 model predictions to demonstrate the good agreement of the measurement with the
 140 predicted $c\bar{c}$ and $b\bar{b}$ contributions.

141 In the case of Au+Au collisions, the e^+e^- mass spectrum shows a very large excess
 142 beyond expectations from hadronic decays in the low mass region between the π^0 and
 143 ω meson masses, as shown in Figure 11 [28]. This excess is dominantly at transverse
 144 momenta below about 1 GeV/c, indicating that it is produced in the cooler late hadronic
 145 phase of the collision.

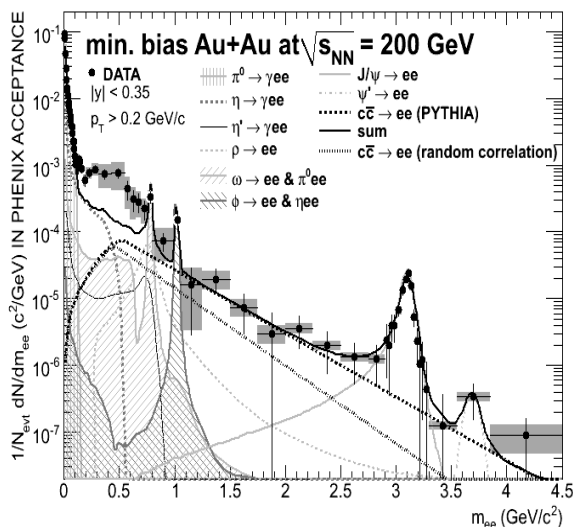


Figure 11. Invariant yield of e^+e^- pairs in minimum bias Au+Au collisions compared to the yield expected from hadronic decays. Statistical (bars) and systematic (boxes) uncertainties are shown separately.

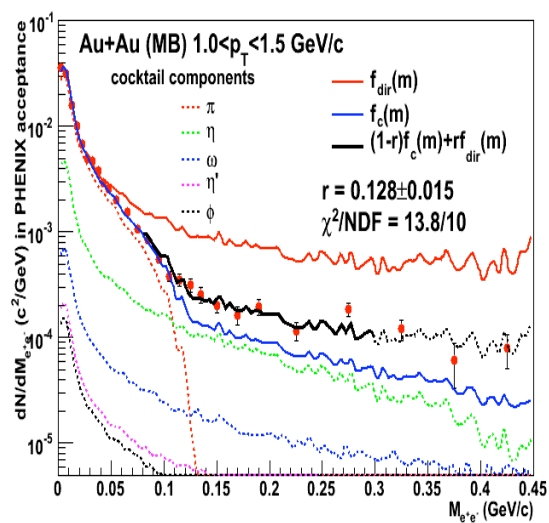


Figure 12. Invariant yield of low mass e^+e^- pairs with $1.0 < p_T < 1.5$ GeV/c in minimum bias Au+Au collisions. The solid blue curve indicates the expectation with the measured η Dalitz contribution.

146 However, a significant e^+e^- excess also persists at higher transverse momenta in
 147 the e^+e^- mass region above the π^0 mass, as seen in Figure 12. This excess can be
 148 used to extract the virtual photon momentum spectrum with an error significantly
 149 smaller, in the low transverse momentum region, than obtained by measurement of real
 150 photons [5, 29, 30, 31]. A small but significant excess is also observed in p+p collisions in
 151 the mass region above the π^0 mass at transverse momenta above 1 GeV/c. As shown in
 152 Figure 13, the measured invariant photon yield for p+p collisions by the virtual photon
 153 measurement is found to be consistent with expectations from pQCD predictions.

154 On the other hand, for Au+Au collisions, the virtual photon yield associated with
 155 the observed e^+e^- excess is greater than that expected from the p+p measurement,
 156 which suggests that it is due to thermal radiation from the early phase of the Au+Au

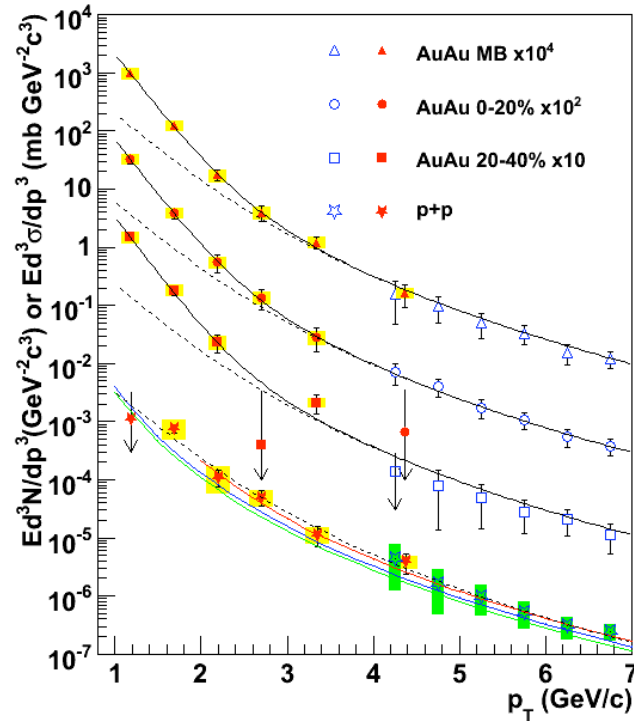


Figure 13. Invariant cross section of direct photons in p+p collisions and Au+Au collisions for several centrality selections compared to scaled NLO pQCD predictions (dashed curves). The open points are previously published PHENIX results [5, 29].

157 collision. These measurements hold promise that the thermal photon spectrum may
 158 finally be extracted with sufficient precision to provide significant constraints on the
 159 initial temperature of the dense matter being created at RHIC [30, 31, 32].

160 References

- 161 [1] "RHIC Scientists Serve Up 'Perfect' Liquid",
 162 http://www.bnl.gov/bnlweb/pubaf/pr/PR_display.asp?prID=05-38
 163 [2] A. Franz (for the PHENIX Collaboration), these proceedings.
 164 [3] A. Adare *et al.*, (PHENIX Collaboration), arXiv:0801.4020.
 165 [4] K. Adcox *et al.*, (PHENIX Collaboration), Phys. Rev. Lett. **88**, 022301 (2002).
 166 [5] S.S. Adler *et al.*, (PHENIX Collaboration), Phys. Rev. Lett. **94**, 232301 (2005).
 167 [6] A. Adare *et al.*, (PHENIX Collaboration), arXiv:0801.4555.
 168 [7] I. Vitev, Phys. Lett. B **639**, 337 (2006).
 169 [8] A. Adare *et al.*, (PHENIX Collaboration), arXiv:0801.1665.
 170 [9] K. Reygers (for the PHENIX Collaboration), these proceedings.
 171 [10] K. Miki (for the PHENIX Collaboration), these proceedings.
 172 [11] S.S. Adler *et al.*, (PHENIX Collaboration), Phys. Rev. **C76**, 034904 (2007).
 173 [12] M. Ngyuen (for the PHENIX Collaboration), these proceedings.
 174 [13] T. Matsui and H. Satz, Phys. Lett. **B 178** (1985) 416.
 175 [14] M.C. Abreu *et al.*, (NA50 Collaboration), Phys. Lett. B **410**, 337 (1997).

- 176 [15] S. Oda (for the PHENIX Collaboration), these proceedings.
177 [16] A. Adare *et al.*, (PHENIX Collaboration), arXiv:0801.0220.
178 [17] A. Adare *et al.*, (PHENIX Collaboration), Phys. Rev. Lett. **98**, 232301 (2007).
179 [18] K.J. Eskola, V.J. Kolhinen, and R. Vogt, Nucl. Phys. **A 696**, 729 (2001).
180 [19] A. Adare *et al.*, (PHENIX Collaboration), arXiv:0711.3917.
181 [20] M. Wysocki (for the PHENIX Collaboration), these proceedings.
182 [21] A. Adare *et al.*, (PHENIX Collaboration), Phys. Rev. Lett. **98**, 172301 (2007).
183 [22] R. Averbeck (for the PHENIX Collaboration), these proceedings.
184 [23] H. van Hees, V. Greco, and R. Rapp, Phys. Rev. **C 73**, 034913 (2006).
185 [24] M. Cacciari, P. Nason, and R. Vogt, Phys. Rev. Lett. **95**, 122001 (2005).
186 [25] D. Hornback (for the PHENIX Collaboration), these proceedings.
187 [26] Y. Morino (for the PHENIX Collaboration), these proceedings.
188 [27] A. Adare *et al.*, (PHENIX Collaboration), Phys. Rev. **C77**, 024912 (2008).
189 [28] S. Afanasiev *et al.*, (PHENIX Collaboration), arXiv:0706.3034.
190 [29] S.S. Adler *et al.*, (PHENIX Collaboration), Phys. Rev. Lett. **98**, 012002 (2007).
191 [30] A. Adare *et al.*, (PHENIX Collaboration), arXiv:0804.4186.
192 [31] T. Dahms (for the PHENIX Collaboration), these proceedings.
193 [32] P.W. Stankus, Ann. Rev. Nucl. Part. Sci. **55** 517 (2005).